

Proportional Integral - Resonant and Dual Loop Current Control Structure Comparison For Grid Connected Converters in the Rotating Frame

Srinivas Gulur*, Vishnu Mahadeva Iyer[†] and Subhashish Bhattacharya[‡]

FREEDM Systems Center, North Carolina State University, Raleigh, USA.

Email: *sgulur@ncsu.edu, [†]vmahade@ncsu.edu, [‡]sbhatta4@ncsu.edu

Abstract—Over the past few years, due the increasing penetration of renewable energy, there has been a steady rise in the harmonic content in grid voltages. In such circumstances, a proportional integral (PI) based current control in the synchronous reference rotating frame (dq) for a grid connected voltage source converter may not be adequate to suppress the harmonic components and to precisely follow the fundamental frequency component with zero steady state error. Several current control structures have been proposed, with proportional integral - resonant controller (PI-RES) based structure being one of the most popular. In this paper, the PI-RES has been compared to the recently introduced dual loop current control structure. Both these current control structures have been compared in terms of their tracking, filtering and disturbance rejection capability. Robustness of both these structures has also been analyzed under a grid impedance variation. Simulation and experimental results have been provided to validate the analysis presented.

Index Terms—current control, dq frame control, resonant controller, grid voltage harmonics, voltage unbalances.

I. INTRODUCTION

Pulse width modulated (PWM) based voltage source converter topologies have emerged as favored power electronic based topologies for integration of renewable energy to utility or micro grids. With considerable rise in the renewable energy integration, there has been an increase in the power quality issues in the grid as well. Stringent restrictions on the quality of grid currents, which can be injected into the grid, have been defined in IEEE 519 [1]. Hence, it is imperative to have a robust current control structure for these voltage source based grid connected converters to operate under non-ideal grid conditions. Since a proportional integral (PI) controller can be used for achieving zero steady state error, regulating the fundamental component of the grid current in the dq frame is conventionally preferred. In reality, the grid voltages contain lower order harmonic components along with the fundamental component. As the grid currents would also contain similar unwanted harmonic components [2], these lower order harmonic components can affect the PI regulator.

Several structures have been proposed in literature for improving the current regulators in the stationary or the synchronous reference frame [3]–[12]. Proportional Integral - Resonant (PI-RES) is one of the popular methods for achieving zero steady state error in the dq frame when the

grid voltages contain unwanted harmonics. This is achieved by using PI and resonant controllers (for each individual harmonic component). Dual loop current control structure is yet another method that was introduced recently to improve the current regulation in the dq frame under non-ideal grid conditions. The dual loop structure uses two controllers, one for reference tracking and the other for improved filtering action and disturbance rejection. In this paper, the PI-RES has been compared with the dual loop current control structure when the grid voltages are unbalanced and contain lower order harmonics. Current control response to load variation and sensitivity to filter parameter robustness under grid impedance variations have also been analyzed.

A brief description of different sections in this paper are given below. Section II describes the PI-RES current control structure and the effects on reference tracking and disturbance rejection due to damped and undamped second order resonant controllers. The dual loop control structure and its associated transfer functions are provided in Section III. Section IV gives a detailed comparison between the PI-RES and dual loop current control structure based on voltage harmonics rejection, load disturbance mitigation and grid impedance variation. Finally, the simulation and experimental results are presented and explained in Section V.

II. PI-RES BASED CURRENT CONTROL STRUCTURE

PI-RES is a popular control structure used for tracking the fundamental current component with zero steady state error, while simultaneously rejecting unwanted current harmonic components in the dq frame [5]. In this structure, $C_{pi}(s)$ is used as a PI controller to track the fundamental current component which appears as dc in dq frame. $C_{rh}(s)$ (h signifies the harmonic number) refers to the resonant controller (RES) used for rejecting the necessary harmonic component as shown in Fig. 1. The current harmonics have to be known a priori in order to design RES controllers tuned at the respective harmonic frequencies. The control feed-forward, grid voltage and load disturbances are described by $V_{f-dis}(s)$, $V_{g-dis}(s)$ and $I_{dis}(s)$, respectively.

Multiple parallel $C_{rh}(s)$ controllers can be added when there exist multiple harmonic current components. A typical

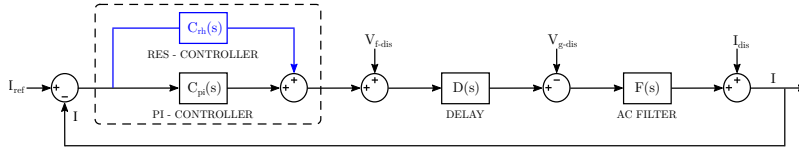


Fig. 1: A PI-RES based current control structure in the dq frame for a voltage source converter [5].

undamped $C_{rh}(s)$ is shown in (1).

$$C_{rh}(s) = \sum_{h=1,2,3..}^n \frac{K_{rh}s}{s^2 + (hw)^2} \quad (1)$$

A modified damped version for digital implementation [13] is described in (2), where w_c refers to the lower breakpoint frequency, w refers to the fundamental frequency component and K_{rh} defines the gain of the resonant function.

$$C_{rh}(s) = \sum_{h=1,2,3..}^n \frac{K_{rh}w_c s}{s^2 + 2w_c s + (hw)^2} \quad (2)$$

Hence, the overall controller for the dq frame current control can be defined as shown in (3).

$$C(s) = \underbrace{\left[K_p + \frac{K_i}{s} \right]}_{C_{pi}(s)} + \underbrace{\sum_{h=1,2,3..}^n \frac{K_{rh}w_c s}{s^2 + 2w_c s + (hw)^2}}_{C_{rh}(s)} \quad (3)$$

For this paper, it has been assumed that the grid voltages are unbalanced and comprise of lower order harmonics, predominantly the 5^{th} and 7^{th} components. Since unbalanced currents propagate as 2^{nd} harmonic components in the dq frame, a RES is required to be tuned to double the line frequency. Similarly, the presence of the 5^{th} and 7^{th} components culminates in a 6^{th} harmonic current in the dq frame, leading to the usage of an additional 6^{th} harmonic RES. Under w_c variations, the associated reference tracking, grid voltage disturbance and load/sensitivity disturbance transfer functions are given in (4),

(5) and (6), respectively.

$$\frac{I(s)}{I_{ref}(s)} \Big|_{I_{dis}(s), V_{f-dis}(s), V_{g-dis}(s)=0} = \frac{[C_{pi}(s) + C_{rh}(s)]D(s)F(s)}{1 + [C_{pi}(s) + C_{rh}(s)]D(s)F(s)} \quad (4)$$

$$\frac{I(s)}{I_{dis}(s)} \Big|_{I_{ref}(s), V_{f-dis}(s), V_{g-dis}(s)=0} = \frac{1}{1 + [C_{pi}(s) + C_{rh}(s)]D(s)F(s)} \quad (5)$$

$$\frac{I(s)}{-V_{g-dis}(s)} \Big|_{I_{ref}(s), V_{f-dis}(s), I_{dis}(s)=0} = \frac{F(s)}{1 + [C_{pi}(s) + C_{rh}(s)]D(s)F(s)} \quad (6)$$

Appropriate selection of w_c is crucial for a robust control strategy. A higher value for w_c would improve the system's insensitivity to grid frequency variation, as shown in Fig. 2 and 3. However, an increase in w_c may degrade the tracking performance by creating low frequency amplification in the reference tracking loop, as shown in Fig. 4a. This would result in an oscillatory response during a step change in the reference current, as shown in Fig. 4b. The controller $C(s)$ has been designed as described in [13] and reference tracking bandwidth has been fixed at $500Hz$, with the two RESs being tuned at 2^{nd} and 6^{th} harmonic frequencies for illustration purposes.

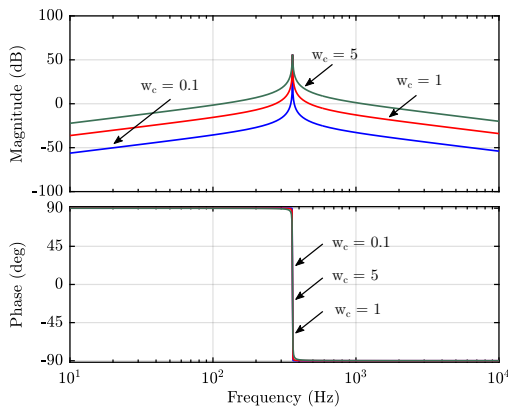


Fig. 2: Effect of w_c variation on $C_{rh}(s)$.

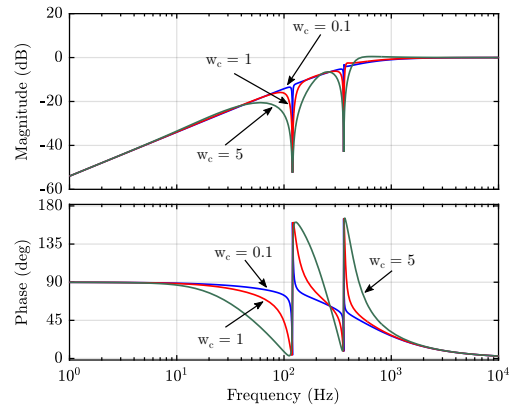


Fig. 3: Load disturbance rejection transfer function for different values of w_c .

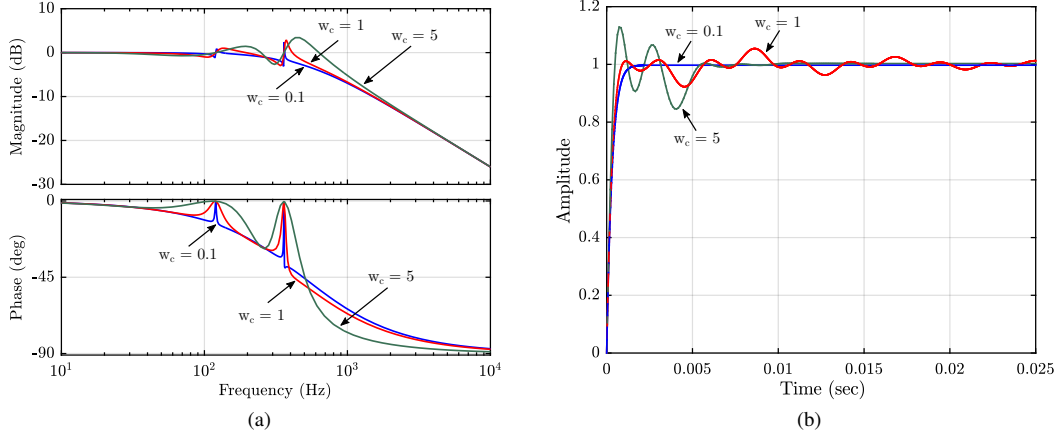


Fig. 4: Variation in w_c for (a) reference tracking transfer functions and (b) its associated step responses.

III. DUAL LOOP CURRENT CONTROL STRUCTURE

A dual loop current control structure [14], based on model based disturbance attenuator [15], shown in Fig. 5, was introduced to eliminate the lower order harmonic components in grid currents by independent control of reference tracking and disturbance rejection in the dq frame. This current control structure can achieve a better disturbance rejection and superior filtering action, without impacting the reference tracking performance. A secondary advantage is that, unlike the PI-RES controller, multiple RES controllers are not required to handle multiple harmonic components. Two controllers, $C_1(s)$ and $C_2(s)$, are sufficient for both reference tracking and disturbance rejection respectively, across all unwanted harmonic frequency components.

$P_m(s) = D_m(s)F_m(s)$ and $P_{ac}(s) = D(s)F(s)$ denote the plant model and the actual plant respectively. $\frac{I(s)}{I_{ref}(s)}$ gives the current reference tracking transfer function.

$$\frac{I(s)}{I_{ref}(s)} \Big|_{I_{dis}(s), V_{f-dis}(s), V_{g-dis}(s)=0} = \frac{C_1(s)P_{ac}(s)[1 + C_2(s)P_m(s)]}{[1 + C_2(s)P_{ac}(s)] + C_1(s)P_{ac}(s)[1 + C_2(s)P_m(s)]} \quad (7)$$

(7) can be reduced to (8) under the assumption that the plant model closely represents the actual plant ($P_m(s) \simeq P_{ac}(s)$).

$$\frac{I(s)}{I_{ref}(s)} = \frac{C_1(s)P_{ac}(s)}{1 + C_1(s)P_{ac}(s)} \quad (8)$$

$\frac{I(s)}{I_{dis}(s)}$ describes the effect of load disturbance, I_{dis} on the output current, I . The output current to load disturbance transfer function can be defined as in (9). Under the condition

($P_m(s) \simeq P_{ac}(s)$), (9) can further be reduced to (10).

$$\frac{I(s)}{I_{dis}(s)} \Big|_{I_{ref}(s), V_{f-dis}(s), V_{g-dis}(s)=0} = \frac{1}{[1 + C_2(s)P_{ac}(s)] + C_1(s)P_{ac}(s)[1 + C_2(s)P_m(s)]} \quad (9)$$

$$\frac{I(s)}{I_{dis}(s)} = \frac{1}{[1 + C_1(s)P_{ac}(s)][1 + C_2(s)P_{ac}(s)]} \quad (10)$$

Similarly, the output current to grid voltage disturbance, V_{g-dis} transfer function can be defined as $\frac{I(s)}{V_{g-dis}(s)}$.

$$\frac{I(s)}{V_{g-dis}(s)} \Big|_{I_{ref}(s), I_{dis}(s), V_{f-dis}(s)=0} = \frac{F(s)}{[1 + C_2(s)P_{ac}(s)] + C_1(s)P_{ac}(s)[1 + C_2(s)P_m(s)]} \quad (11)$$

$$\frac{I(s)}{-V_{g-dis}(s)} = \frac{F(s)}{[1 + C_1(s)P_{ac}(s)][1 + C_2(s)P_{ac}(s)]} \quad (12)$$

A simplified expression described by (12) can be deduced under the assumption that the plant model matches with the actual plant ($P_m(s) \simeq P_{ac}(s)$). $C_1(s)$ and $C_2(s)$ are chosen as proportional- integral (PI) and proportional (P) controllers, respectively. These controllers are designed as suggested in [14]. It is interesting to note from Fig. 6 that when the disturbance rejection controller, $C_2(s)$ values ($C_2(s)$ is chosen as a simple gain) are varied, the reference tracking function or the step response of the dual loop control structure are unaffected as the reference tracking is decoupled from disturbance rejection.

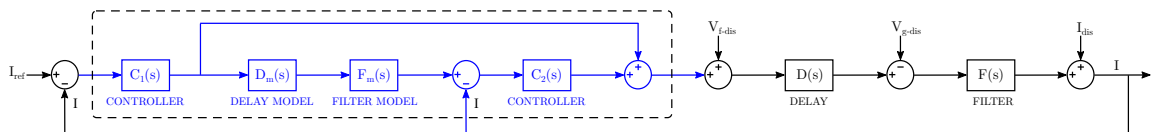


Fig. 5: A dual loop based current control structure for voltage source converter in the dq frame [14].

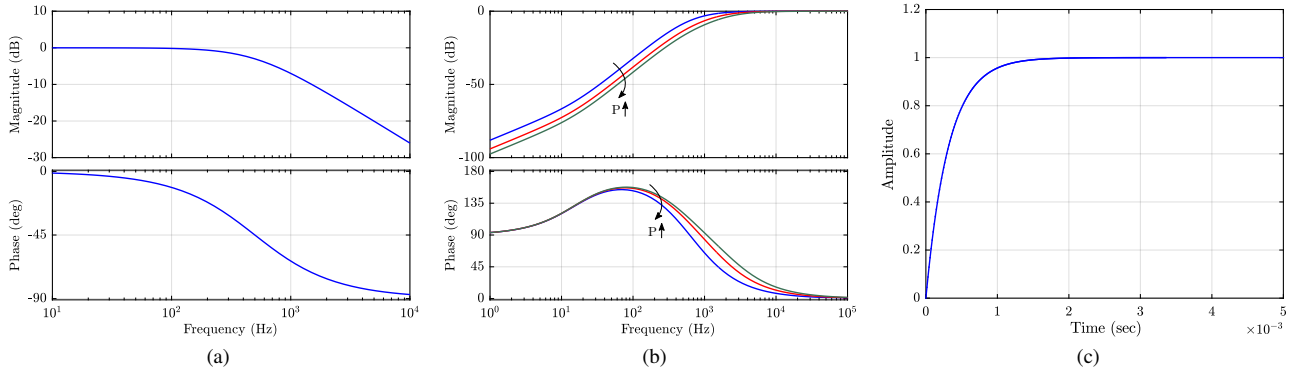


Fig. 6: Dual loop plots for (a) reference tracking capability (b) load disturbance rejection capability (c) associated step response.

IV. COMPARISON BETWEEN PI-RES AND DUAL LOOP CURRENT CONTROL STRUCTURES

The PI-RES and dual loop based current control schemes have been compared based on their ability to accurately track reference changes, rejection of grid voltage disturbances and load disturbances, and robustness to grid impedance variation. This has been achieved by using a grid interfaced voltage source converter with an inductive L filter, and a conventional synchronous reference frame phase locked loop (SRF-PLL) [16]. The circuit and control parameters are given in Table I.

TABLE I: Voltage Source Converter Parameters

Parameter	Value
Grid Frequency, f_g	60 Hz
AC filter inductance, L	2 mH
AC filter resistance, R_L	0.2 Ω
Switching frequency, f_{sw}	20 kHz
Reference tracking bandwidth - Dual Loop	500 Hz
Proportional gain for $C_2(s)$ - Dual Loop	30.0
Reference tracking bandwidth - PI-RES	500 Hz
Resonant controllers (RESs)	120 and 360 Hz
SRF-PLL bandwidth	10 Hz

A. Reference Tracking Capability

As observed from Fig. 7a, the dual loop structure does not show any low frequency amplification while the PI-RES contains low frequency amplification at the the 2nd and 6th harmonic frequencies due to the usage of resonant controllers. This low frequency amplification may generate oscillations during a step response and lead to stability issues in a practical system.

B. Grid Voltage Harmonic Rejection

Ideally, the PI-RES can provide infinite attenuation at the required harmonic frequencies. Practically, this capability gets affected by the digital implementation of such second harmonic controllers (RES). Any type of delays due to computation or PWM may cause a slight variation in the actual harmonic frequency of the RES. The digital implementation adds additional damping which will limit the maximum attenuation achievable. On the other hand, the dual loop can only provide moderate attenuation at the required harmonic frequencies with the choice of a simple proportional controller for $C_2(s)$. It may be noted that a different controller form can be selected for $C_2(s)$ for improving the attenuation performance. While it can be seen in Fig. 7b that the PI-RES has a better attenuation for the 2nd and 6th harmonic, the dual loop has a superior voltage harmonic attenuation across frequencies. Though both

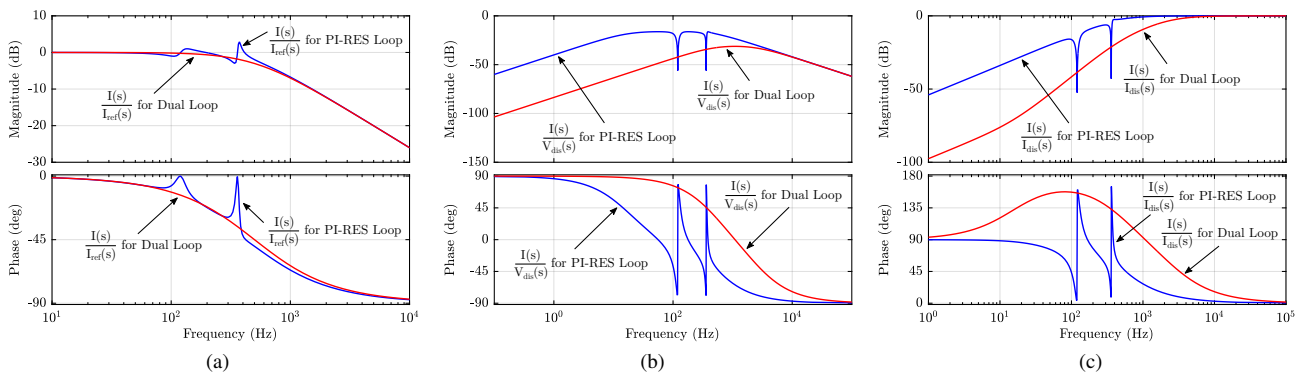


Fig. 7: Comparison between PI-RES and dual loop (a) reference tracking capability (b) voltage harmonic rejection capability (c) load disturbance rejection capability.

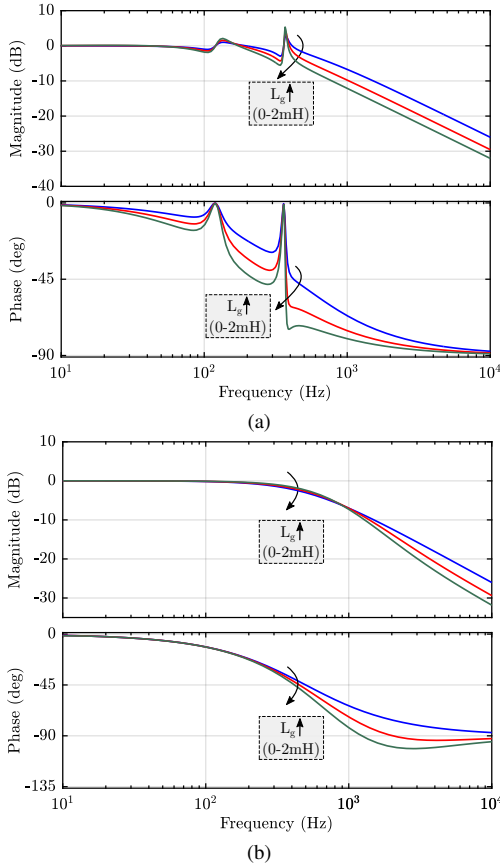


Fig. 8: Closed loop reference tracking plots under grid impedance variation for (a) PI-RES structure (b) Dual loop structure where L_g refers to grid inductance.

the control methods require a PLL for grid synchronization and unit vector generation, an adaptive PI-RES requires the frequency generated from the PLL to be precise leading to an increase in the design and implementation complexity of the PLL.

C. Load Disturbance Rejection

Fig. 7c compares the load disturbance rejection transfer function of both control methods. The dual loop current control structure can mitigate any type of a load disturbance as compared to the PI-RES as its load disturbance rejection function has a higher attenuation across the frequency range.

D. Effect of Grid Impedance Variation

It can be observed in Fig. 8a and 8b that under a severe grid inductance variation, there is minimal degradation in the bandwidth of the dual loop current control structure, as compared to the PI-RES due to its superior sensitivity function ($S(s)$). The relationship between the robustness to parametric variation and sensitivity can be given by (13), where $P(s)$, $\delta P(s)$, $I(s)$ and $\delta I(s)$ refer to the plant, variation in plant,

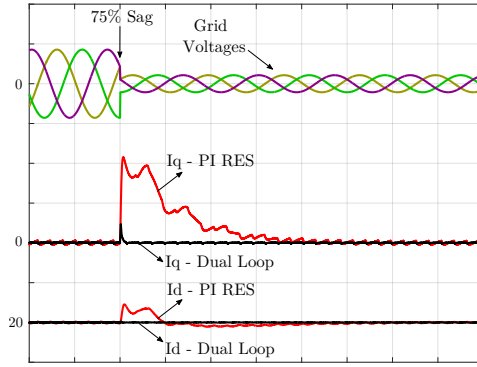


Fig. 9: Disturbance rejection capability of PI-RES and dual loop under 75% balanced grid voltage (line to line) sag. Scale: Line voltages [100V/div], dq currents [3A/div] and time [10ms/div]

output current and the variation in output current, respectively.

$$\delta I(s) \simeq \left[S(s) \right] \left[\frac{\delta P(s)}{P(s)} \right] I(s) \quad (13)$$

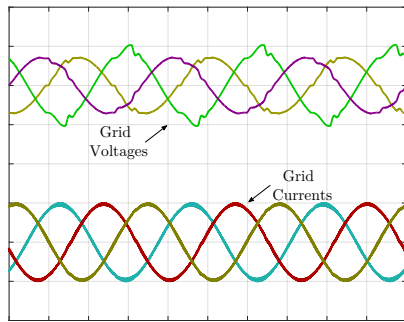
From equation (13), it can be observed that if $S(s)$ is low at the lower frequencies, then the effect due to $\delta P(s)$ on $\delta I(s)$ will be negligible. Since there is a bandwidth degradation in the PI-RES control structure with grid inductance variation, the system may run into stability issues if the voltage source converter contains an outer loop in addition to the inner current loop.

V. RESULTS AND DISCUSSION

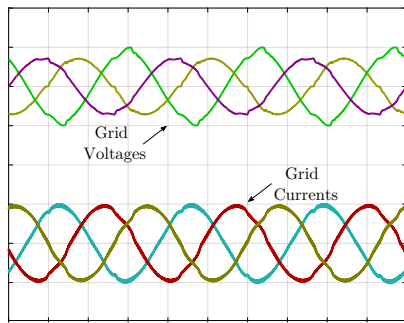
For the sake of performance comparison of the PI-RES and the dual loop current control structures, various simulation and experimental results are presented. For all simulations and experiments, the voltage source converter parameters are based on Table I.

To compare the disturbance rejection feature under abnormal grid conditions and during faults, a 75% symmetrical sag was introduced in the grid voltages. Fig. 9 compares the I_d and I_q current transients from a circuit simulation. It can be seen that the current transients are minimal with the dual loop current control structure owing to its superior sensitivity functions as shown in Fig. 7b and 7c.

Another test scenario is presented, wherein unbalances and lower order harmonics are intentionally introduced in the grid voltages. A circuit simulation was performed to evaluate the two control structures. With a polluted grid, it is observed that the the dual loop structure is capable of assisting the voltage source converter for injection of balanced fundamental currents to the grid, as shown in Fig. 10a. Even the PI-RES controller with a 2^{nd} harmonic RES performs well under distorted grid voltages, but the grid current distortion is slightly higher than that of the dual loop controller based implementation as seen in Fig. 10b. As discussed in Section



(a)



(b)

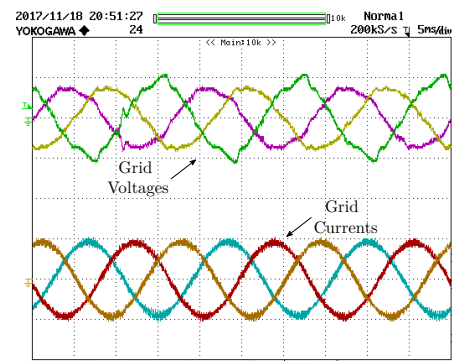
Fig. 10: Simulation results with distorted grid voltages (line-line) [100V/div] and grid currents [10A/div] versus time [5ms/div] for the (a) Dual Loop structure (b) PI-RES structure.

II, multiple RES controllers are needed to perfectly reject all lower order harmonics.

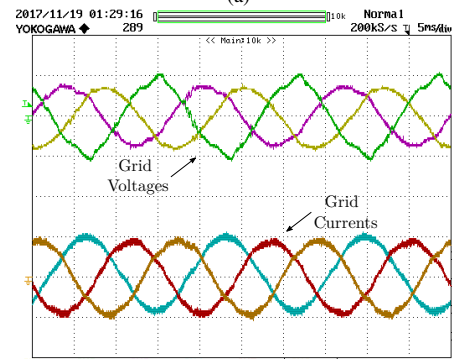
This was further validated by experiments conducted on a 2-level, 3ϕ voltage source converter prototype. The experimental results are in agreement with the simulation results as can be seen from Fig. 11. With the PI-RES controller implementation, although there is an RES at the 2^{nd} harmonic frequency, it can be observed that line currents are still slightly unbalanced in Fig. 11b. This imbalance is attributed to the non-adaptive nature of the RES implementation. The RES is always tuned to 120 Hz and there will be minor variations in the actual grid frequency from 60 Hz which can affect the attenuation offered by 2^{nd} harmonic RES. This was intentionally done to showcase the effect of variation of the grid frequency on RES performance. Although, the RES could have been made adaptive, the frequency generated by the PLL itself would be polluted due to the distorted voltages leading to the RES performance not being satisfactory.

VI. CONCLUSION

PI-RES and dual loop current control structures have been analyzed in-terms of their reference tracking, voltage harmonic filtering and disturbance rejection capability. It is shown that although the PI-RES structure can provide higher attenuation at specific voltage harmonic frequencies, it is subject to low frequency disturbance/noise amplifications in its reference



(a)



(b)

Fig. 11: Experimental results with distorted grid voltages (line-line) [100V/div] and grid currents [10A/div] versus time [5ms/div] for the (a) Dual Loop structure (b) PI-RES structure.

tracking function, alongwith poor load rejection capability. The dual loop not only provides good attenuation across a wide range of voltage harmonic frequencies, but also provides excellent load disturbance rejection capability. Each RES in the PI-RES can cancel out only a single harmonic frequency in the dq frame, unlike the dual loop which uses only a single disturbance rejection controller across a wide range of harmonic frequencies. The dual loop can also provide improved robustness under a grid impedance variation due to its superior sensitivity function. Simulation and experimental results showing the dq and ac currents for both the PI-RES and dual loop based structure have been provided under abnormal and/or severely distorted grid voltage conditions to validate the analysis presented.

REFERENCES

- [1] "IEEE Recommended Practice and Requirements for Harmonic Control in Electric Power Systems - Redline," *IEEE Std 519-2014 (Revision of IEEE Std 519-1992) - Redline*, pp. 1–213, June 2014.
- [2] R. Teodorescu, F. Blaabjerg, M. Liserre, and P. C. Loh, "Proportional-resonant controllers and filters for grid-connected voltage-source converters," *IEE Proceedings - Electric Power Applications*, vol. 153, no. 5, pp. 750–762, September 2006.
- [3] P. Mattavelli, "A closed-loop selective harmonic compensation for active filters," *IEEE Transactions on Industry Applications*, vol. 37, no. 1, pp. 81–89, Jan 2001.
- [4] S. Fukuda and T. Yoda, "A novel current-tracking method for active filters based on a sinusoidal internal model [for PWM invertors]," *IEEE*

- Transactions on Industry Applications*, vol. 37, no. 3, pp. 888–895, May 2001.
- [5] M. Liserre, R. Teodorescu, and F. Blaabjerg, “Multiple harmonics control for three-phase grid converter systems with the use of PI-RES current controller in a rotating frame,” *IEEE Transactions on Power Electronics*, vol. 21, no. 3, pp. 836–841, May 2006.
- [6] M. Xue, Y. Zhang, Y. Kang, Y. Yi, S. Li, and F. Liu, “Full feedforward of grid voltage for discrete state feedback controlled grid-connected inverter with lcl filter,” *IEEE Transactions on Power Electronics*, vol. 27, no. 10, pp. 4234–4247, Oct 2012.
- [7] E. Wu and P. W. Lehn, “Digital current control of a voltage source converter with active damping of lcl resonance,” *IEEE Transactions on Power Electronics*, vol. 21, no. 5, pp. 1364–1373, Sept 2006.
- [8] J. Dannehl, F. W. Fuchs, and P. B. Thgersen, “PI State Space Current Control of Grid-Connected PWM Converters With LCL Filters,” *IEEE Transactions on Power Electronics*, vol. 25, no. 9, pp. 2320–2330, Sept 2010.
- [9] I. J. Gabe, V. F. Montagner, and H. Pinheiro, “Design and implementation of a robust current controller for vsi connected to the grid through an lcl filter,” *IEEE Transactions on Power Electronics*, vol. 24, no. 6, pp. 1444–1452, June 2009.
- [10] M. Ebrahimi, S. A. Khajehoddin, and M. Karimi-Ghartemani, “Fast and robust single-phase dq current controller for smart inverter applications,” *IEEE Transactions on Power Electronics*, vol. 31, no. 5, pp. 3968–3976, May 2016.
- [11] Y. Yang, K. Zhou, H. Wang, F. Blaabjerg, D. Wang, and B. Zhang, “Frequency adaptive selective harmonic control for grid-connected inverters,” *IEEE Transactions on Power Electronics*, vol. 30, no. 7, pp. 3912–3924, July 2015.
- [12] F. Gonzalez-Espin, G. Garcera, I. Patrao, and E. Figueres, “An adaptive control system for three-phase photovoltaic inverters working in a polluted and variable frequency electric grid,” *IEEE Transactions on Power Electronics*, vol. 27, no. 10, pp. 4248–4261, Oct 2012.
- [13] D. N. Zmood, D. G. Holmes, and G. H. Bode, “Frequency-domain analysis of three-phase linear current regulators,” *IEEE Transactions on Industry Applications*, vol. 37, no. 2, pp. 601–610, Mar 2001.
- [14] S. Gulur, V. M. Iyer, and S. Bhattacharya, “A dual loop current control structure with improved disturbance rejection for grid connected converters in the synchronous rotating reference frame,” *IEEE Energy Conversion Congress and Exposition*, 2017.
- [15] B.-K. Choi, C.-H. Choi, and H. Lim, “Model-based disturbance attenuation for cnc machining centers in cutting process,” *IEEE/ASME Transactions on Mechatronics*, vol. 4, no. 2, pp. 157–168, Jun 1999.
- [16] V. Kaura and V. Blasko, “Operation of a phase locked loop system under distorted utility conditions,” *IEEE Transactions on Industry Applications*, vol. 33, no. 1, pp. 58–63, Jan 1997.